Oncogene (2016) **35**, 4641–4652

www.nature.com/onc

ORIGINAL ARTICLE

Overexpression of *PIK3CA* in murine head and neck epithelium drives tumor invasion and metastasis through PDK1 and enhanced TGFβ signaling

L Du[1,2,9], X Chen[1,9], Y Cao[1,3], L Lu[1], F Zhang[1], S Bornstein[4], Y Li[4], P Owens[4], S Malkoski[5], S Said[6], F Jin[3], M Kulesz-Martin[7], N Gross[4], X-J Wang[6] and S-L Lu[1,6,8]

Head and neck squamous cell carcinoma (HNSCC) patients have a poor prognosis, with invasion and metastasis as major causes of mortality. The phosphatidylinositol 3-kinase (PI3K) pathway regulates a wide range of cellular processes crucial for tumorigenesis, and *PIK3CA* amplification and mutation are among the most common genetic alterations in human HNSCC. Compared with the well-documented roles of the PI3K pathway in cell growth and survival, the roles of the PI3K pathway in tumor invasion and metastasis have not been well delineated. We generated a *PIK3CA* genetically engineered mouse model (*PIK3CA-GEMM*) in which wild-type *PIK3CA* is overexpressed in head and neck epithelium. Although *PIK3CA* overexpression alone was not sufficient to initiate HNSCC formation, it significantly increased tumor susceptibility in an oral carcinogenesis mouse model. *PIK3CA* overexpression in mouse oral epithelium increased tumor invasiveness and metastasis by increasing epithelial–mesenchymal transition and by enriching a cancer stem cell phenotype in tumor epithelial cells. In addition to these epithelial alterations, we also observed marked inflammation in tumor stroma. AKT is a central signaling mediator of the PI3K pathway. However, molecular analysis suggested that progression of *PIK3CA*-driven HNSCC is facilitated by 3-phosphoinositide-dependent protein kinase (PDK1) and enhanced transforming growth factor β (TGFβ) signaling rather than by AKT. Examination of human HNSCC clinical samples revealed that both PIK3CA and PDK1 protein levels correlated with tumor progression, highlighting the significance of this pathway. In summary, our results offer significant insight into how *PIK3CA* overexpression drives HNSCC invasion and metastasis, providing a rationale for targeting PI3K/PDK1 and TGFβ signaling in advanced HNSCC patients with *PIK3CA* amplification.

Oncogene (2016) **35,** 4641–4652; doi:10.1038/onc.2016.1; published online 15 February 2016

INTRODUCTION

Head and neck squamous cell carcinoma (HNSCC) is the sixth most common cancer worldwide, with 650 000 new cases and 350 000 deaths every year.[1] There are 55 000 new cases and over 15 000 deaths from HNSCC annually in the United States.[2] The most common etiological factors for HNSCC are tobacco exposure, alcohol and human papilloma virus infection.[3] Although tremendous efforts have been made to improve the treatment for HNSCC patients, HNSCC remains a lethal disease, with 5-year survival rates below 50%, a number that has not significantly changed in several decades.[2] Locoregional invasion, recurrence and metastasis are largely responsible for the poor prognosis of HNSCC patients. However, the underlying molecular mechanisms for HNSCC progression are still poorly understood.

The phosphatidylinositol 3-kinase (PI3K) signaling pathway is a key mediator of cell survival, growth and metabolism, and is commonly altered in many human malignancies, including HNSCC.[4–6] The PI3K family is comprised of three subclasses of lipid kinases. Class IA PI3K, composed of a heterodimer between a p110 catalytic subunit and a p85 regulatory subunit, has been intensively studied and demonstrated to be commonly altered in human cancers.[4,5] PI3K phosphorylates phosphotidylinositol-4,5, bisphosphate to phosphotidylinositol-3,4,5,trisphosphate, a reaction which is antagonized by the tumor-suppressor phosphatase and tensin homolog (PTEN). In turn, phosphotidylinositol-3,4,5, trisphosphate binds a subset of pleckstrin homology domain-containing proteins, including AKT and 3-phosphoinositide-dependent protein kinase (PDK1). AKT is activated by phosphorylation on serine 473 by the mTORC2 complex, and on threonine 308 by PDK1. Activated AKT directly regulates multiple downstream molecules, such as mTORC1 and p70-S6, to transduce the major downstream PI3K signal pathway.[4,5] However, it has been shown that, in certain contexts, PI3K signaling and AKT activation can be uncoupled.[7–9]

Recent exome sequencing in human HNSCC samples revealed that molecular alterations in the PI3K pathway are the most common genetic changes in HNSCC patients' cells.[10–12] Among those changes, *PIK3CA*, the gene coding for the p110α catalytic subunit of PI3K, is most frequently altered through either gene amplification or gain-of-function mutations.[10–12] Over 40% of

[1]Department of Otolaryngology, University of Colorado Anschutz Medical Campus, Aurora, CO, USA; [2]Department of Otolaryngology, Fourth University Hospital of China Medical University, Shengyang, China; [3]Department of Surgical Oncology, The First University Hospital of China Medical University, Shengyang, Liaoning, China; [4]Department of Otolaryngology, Oregon Health and Science University, Portland, OR, USA; [5]Department of Medicine, University of Colorado Anschutz Medical Campus, Aurora, CO, USA; [6]Department of Pathology, University of Colorado Anschutz Medical Campus, Aurora, CO, USA; [7]Department of Dermatology, Oregon Health and Science University, Portland, OR, USA and [8]Department of Dermatology, University of Colorado Anschutz Medical Campus, Aurora, CO, USA. Correspondence: Professor S-L Lu, Department of Otolaryngology, University of Colorado Anschutz Medical Campus, 12700 E 19th Avenue, Mail Stop 8606, Aurora, CO 80045, USA.
E-mail: shi-long.lu@ucdenver.edu
[9]These authors contributed equally to this work.
Received 16 March 2015; revised 15 December 2015; accepted 18 December 2015; published online 15 February 2016

HNSCC cases exhibit *PIK3CA* amplification, and ~10% harbor *PIK3CA* gain-of-function mutations.[4–6,10–13] Although several studies suggest *PIK3CA* alterations correlate with advanced HNSCC stage,[10,14,15] vascular invasion[16] and lymph node metastasis,[17] there are no *in vivo* studies that have elucidated the mechanisms by which *PIK3CA* alterations lead to HNSCC development and progression.

To address this, we generated an inducible head-and-neck-specific genetically engineered mouse model (GEMM), in which *PIK3CA* is overexpressed in head and neck epithelium. Our results showed that in this GEMM overexpression of *PIK3CA* alone resulted in head and neck epithelial hyperplasia but was not sufficient to initiate tumorigenesis. However, overexpression of *PIK3CA* significantly increased susceptibility to oral carcinogen-induced head and neck tumorigenesis. Strikingly, *PIK3CA* overexpression promoted HNSCC invasion and metastasis through epithelial–mesenchymal transition (EMT) and enrichment of putative head and neck cancer stem cells (CSCs). Further molecular studies showed that activation of PDK1 and enhanced transforming growth factor β (TGFβ) signaling play an important part in HNSCC progression. Our findings highlight the key role of PDK1 and TGFβ signaling in HNSCC invasion and metastasis, and suggest that targeting PDK1 and TGFβ signaling may be effective approaches to controlling HNSCC progression, particularly in patients with *PIK3CA* gene amplification.

RESULTS

Overexpression of PIK3CA in murine head and neck epithelia resulted in increased susceptibility to head and neck carcinogenesis

Although *PIK3CA* amplification/mutation has been described in human HNSCC, little is known about its *in vivo* role during head and neck tumorigenesis. To this end, we developed an inducible, head-and-neck-specific *PIK3CA* genetically engineered mouse model (*PIK3CA*-GEMM) using previously published methods.[18] Briefly, the *PIK3CA*-GEMM consists a transactivator mouse line (*K5.GLp65*) and a target mouse line (*tata.PIK3CA*; Figure 1a). In the transactivator line, the keratin 5 (K5) promoter is used to restrict expression of the GLp65 fusion protein to the basal layer of stratified epithelia (for example, buccal mucosa, tongue). GLp65 consists of a GAL4 DNA-binding domain, the NF-κB p65 transactivation domain and an RU486-inducible truncated progesterone receptor ligand-binding domain (ΔPR-LBD). The *K5.GLp65* mice were bred to the *tata.PIK3CA* mice to generate the bigenic *K5.GLp65/tataPIK3CA* (hereafter referred to as *PIK3CA*-

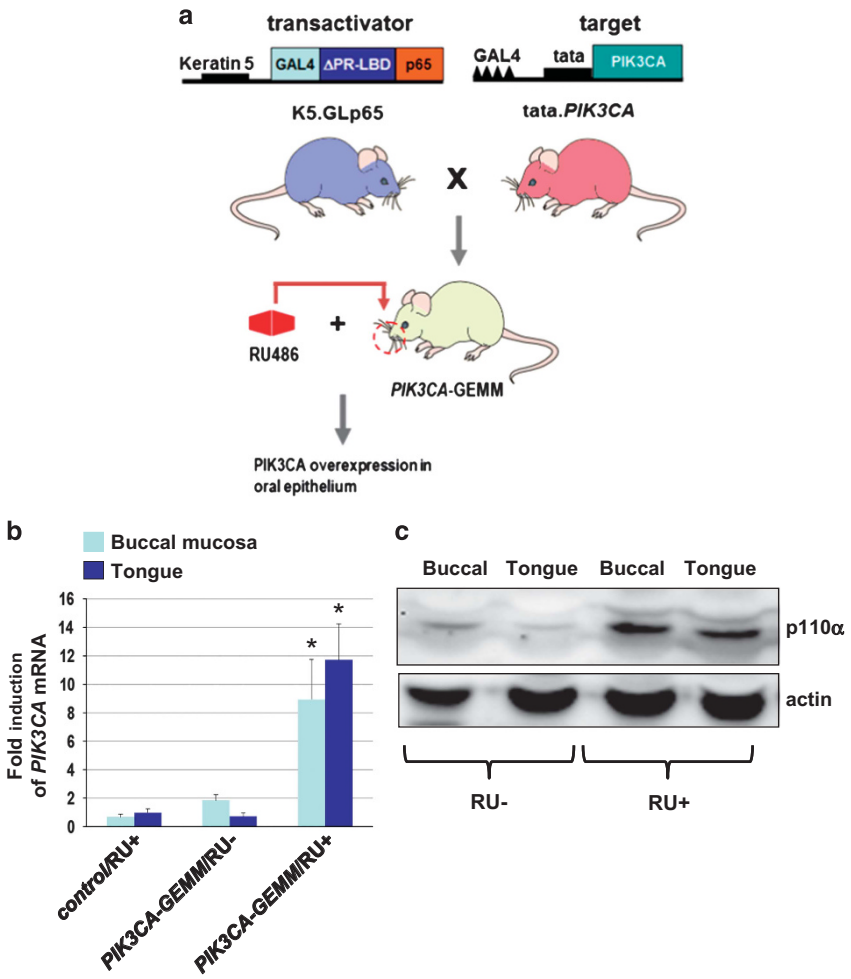

Figure 1. Generation and characterization of the inducible, head-and-neck-specific *PIK3CA* genetically engineered mouse model (*PIK3CA*-GEMM). (**a**) Schematic of generating the *PIK3CA*-GEMM by breeding the transactivator mouse line *K5.GLp65* to the target mouse line tata. *PIK3CA*. (**b**) Fold inductions of the *PIK3CA* mRNA quantified by qRT–PCR using transgene-specific primers. RU = RU486, $n = 6$, $^*P < 0.05$. (**c**) Western blot analysis on protein lysates from the buccal mucosa and tongue of the *PIK3CA*-GEMMs.

GEMM). The monogenic *K5.GLp65* and *tata.PIK3CA* mouse lines were used as experimental controls. Starting at 4 week of age, mice were orally treated with RU486 dissolved in sesame oil. As shown in Figure 1b, upon RU486 application, the expression level of *PIK3CA* mRNA increased about 8- to 10-fold in the buccal mucusa and tongue tissues from the *PIK3CA*-GEMM compared with those from the control mice or the *PIK3CA*-GEMM without RU486 application. Correspondingly, the protein level of p110α (encoded by the *PIK3CA* gene) was also increased in *PIK3CA*-GEMM head and neck tissues upon RU486 application (Figure 1c).

After verifying induced expression of *PIK3CA* in the *PIK3CA*-GEMM head and neck epithelia following RU486 administration, we treated *PIK3CA*-GEMMs with oral RU486 (20 μg/mouse) twice weekly. Epithelial hyperplasia and carcinoma *in situ* with increased cell proliferation were observed in both buccal mucosa and tongue tissue as early as 6 months after initiation of treatment (Supplementary Figure 1). However, these premalignant lesions failed to progress into squamous cell carcinomas (SCCs), suggesting that *PIK3CA* overexpression alone is not sufficient to induce HNSCC formation.

One of the major etiological factors of human HNSCC development is tobacco exposure.[3] To mimic this human situation and investigate the interaction between environmental factors and genetic susceptibility, we applied the 4-nitroquinoline 1 oxide (4NQO)-induced HNSCC carcinogenesis protocol to the *PIK3CA*-GEMM. 4NQO is a DNA adduct-forming agent widely used as a tobacco surrogate to induce HNSCC in mouse models.[19] As shown in Figure 2a, *PIK3CA*-GEMM and control mice were treated with RU486 applied orally twice weekly and with 4NQO added to drinking water (50 μg/ml) starting when the mice were 1-month

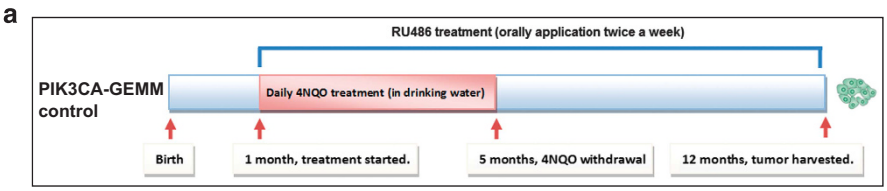

b

Incidence of tumors

Age of mice	control	*PIK3CA*-GEMM
5-6 month	2/25 (8%)	9/23 (39%)*
10-12 month	25/25 (100%)	23/23 (100%)

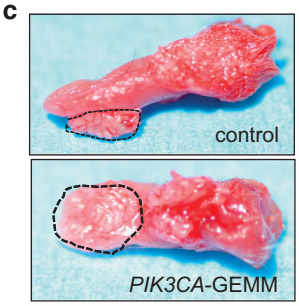

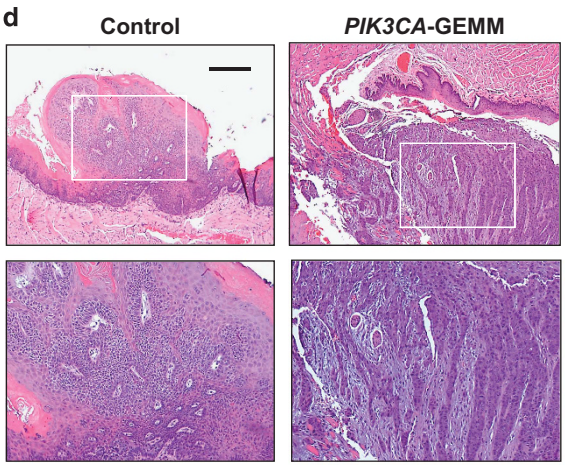

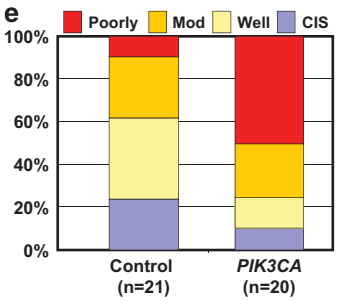

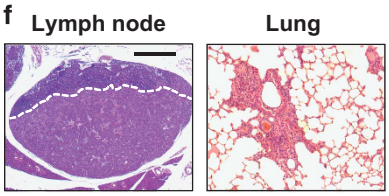

Figure 2. Overexpression of *PIK3CA* together with 4NQO treatment increases tumor susceptibility and promotes tumor invasion and metastasis of the 4NQO-induced HNSCC. (**a**) Schematics of the animal experiment. Starting at 1 month of age, *PIK3CA*-GEMMs and control mice were given 4NQO (50 μg/ml) in the drinking water for 16 weeks, and RU486 (20 μg/mouse) applied orally twice weekly until harvesting mice at 12 months. (**b**) Summary of tumor incidences in the *PIK3CA*-GEMMs and control mice. All mice underwent a biweekly full oral cavity examination, and any pathologic changes were documented. Tumor onset was significantly earlier for the *PIK3CA*-GEMMs (5–6 months) than for the control mice. $*P < 0.01$. (**c**) Gross morphology of tongue SCCs from control mice (upper) and *PIK3CA*-GEMMs (lower). Dotted lines delineate the tumor boundary. Note that tumors from the control mice are papilloma-like, whereas those from the *PIK3CA*-GEMMs are flat. (**d**) Hematoxylin and eosin (H&E) staining of representative tongue tumors shows that tumors from control mice have an out-growth pattern with intact basement membrane (upper left panel), and are well-differentiated (lower left panel), whereas tumors from the *PIK3CA*-GEMMs have a down-growth pattern, with invasion to the tongue muscle (upper right panel), and are poorly differentiated (lower right panel). Scale bar: 100 μm for upper panel, and 25 μm for lower panel. (**e**) Histopathological summary of oral tumors from control mice and *PIK3CA*-GEMMs. CIS, carcinoma *in situ;* Mod, moderately differentiated tumors; Poorly, poorly differentiated tumors; Well, well-differentiated tumors. (**f**) H&E staining of representative lymph node and lung metastases. Dotted line delineates the upper boundary of the tumor. Scale bar: 100 μm.

old. Mice were exposed to 4NQO for 16 weeks, and received RU486 through the end of the 12-month experiment. *PIK3CA* overexpression significantly enhanced susceptibility to 4NQO-induced head and neck carcinogenesis (Figure 2b). By 5 to 6 months of age, 39% of *PIK3CA*-GEMMs developed HNSCC, compared with only 8% of control mice ($P < 0.01$). By 10–12 months, all 4NQO-treated control and *PIK3CA*-GEMM mice developed HNSCC. The authentication of the *PIK3CA* tumors was validated by transgene-specific genotyping PCR (Supplementary Figure 2). By the time of tumor harvest, there were no differences in the general health and nutritional status (for example, activity or body weight) between the control mice and the *PIK3CA*-GEMMs.

Overexpression of PIK3CA in murine head and neck epithelia promotes tumor invasion and metastasis

It was immediately clear that tumors from *PIK3CA*-GEMMs and those from control mice differed in gross appearance: although most control tumors were papillomatous, tumors from the *PIK3CA*-GEMMs were flat (Figure 2c). Histologically, the majority of the control tumors had an out-growth pattern with intact basement membranes (left panels of Figure 2d and Supplementary Figure 3), whereas tumors from the *PIK3CA*-GEMMs predominantly had a down-growth pattern with broken basement membranes and invasion into muscle (right panels of Figure 2d and Supplementary Figure 3). Although over 60% of the control tumors were well-differentiated or carcinoma *in situ*, over 50% of the *PIK3CA*-overexpressing tumors were poorly differentiated as confirmed by a head and neck pathologist (Figures 2d and e and Supplementary Figure 3). Notably, metastases were observed in ~40% of the *PIK3CA*-GEMMs (regional lymph node or lung metastases) compared with no metastases in control mice (Figure 2f). These data showed that overexpression of *PIK3CA* promoted 4NQO-induced HNSCC progression, particularly tumor invasion and metastasis.

PIK3CA overexpression induced de-differentiation, EMT and enriched CSC properties

The poorly differentiated tumor histology observed in the *PIK3CA*-GEMMs was further confirmed by immunostaining of several

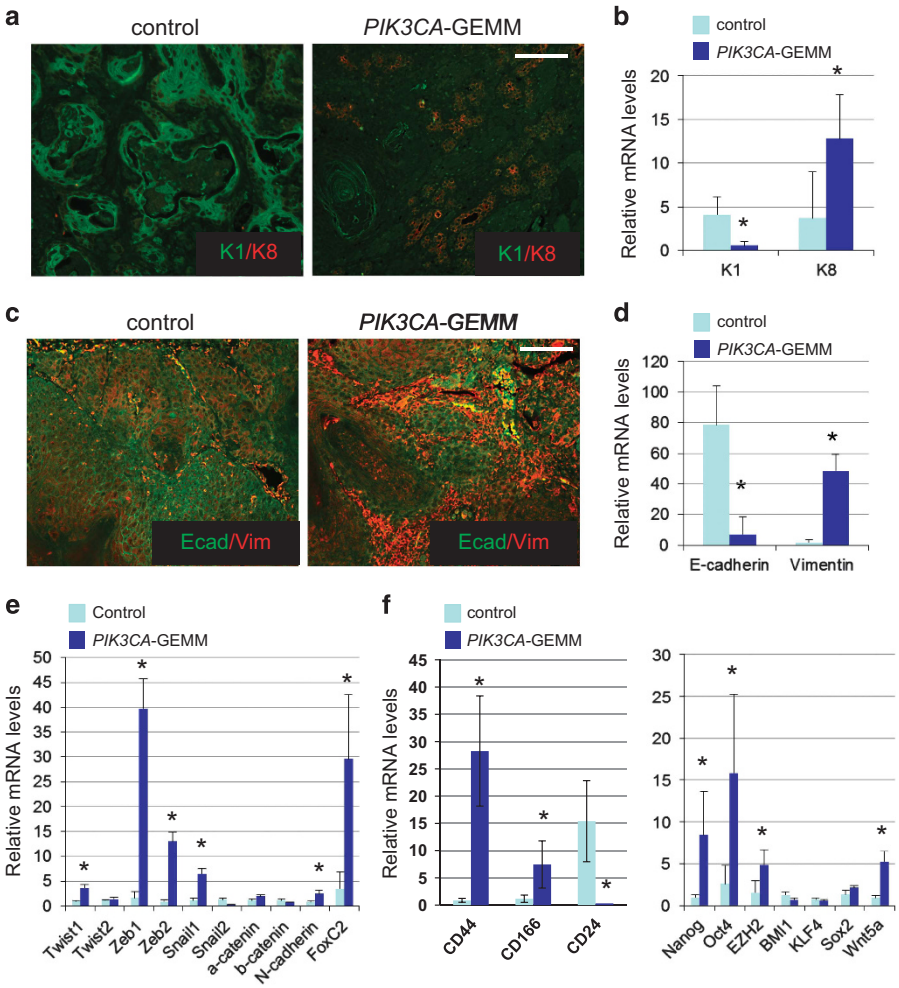

Figure 3. *PIK3CA* overexpression in tumor tissue promotes cellular de-differentiation, epithelial-mesenchymal transition (EMT) and enrichment of cancer stem cell properties. (**a**) Double immunofluorescence (IF) staining of keratin 1 (K1, green) and keratin 8 (K8, red) markers on tongue tumor samples from control mice and *PIK3CA*-GEMMs ($n = 7$). K1 indicates well-differentiated cells, whereas K8 indicates poorly differentiated cells. Scale bar: 25 μm. (**b**) Relative mRNA levels of K1 and K8 measured by qRT–PCR, normalized to β-actin. Results are averages of triplicate experiments. *$P < 0.05$ ($n = 6$ for each group). (**c**) Double IF staining of epithelial marker E-cadherin (green) and mesenchymal marker Vimentin (red) on tongue tumor samples from control mice and *PIK3CA*-GEMMs ($n = 12$). Scale bar: 25 μm. (**d**) Relative mRNA levels of E-cadherin and Vimentin measured by qRT–PCR, normalized to β-actin. Results are averages of triplicate experiments. *$P < 0.05$ ($n = 6$ for each group). (**e**) Relative mRNA levels of EMT-related molecules measured by qRT–PCR, normalized to β-actin. Results are averages of triplicate experiments. *$P < 0.05$ ($n = 6$ for each group). (**f**) Relative mRNA levels of putative markers for cancer stem cell of HNSCC (left panel) and molecules regulating CSC phenotype (right panel) measured by qRT–PCR. Results are averages of triplicate experiments. *$P < 0.05$ ($n = 6$ for each group).

differentiation markers. As shown in Figure 3a, while Keratin 1 (K1, green) was still retained in the control tumors, marking well-differentiated SCC, it was lost in the *PIK3CA*-GEMM tumors. In contrast, Keratin 8 (K8, red), seen in poorly differentiated SCC, was rarely expressed in control tumors, whereas it was highly expressed in tumors from *PIK3CA*-GEMMs. This differential keratin expression was further confirmed by K1 and K8 mRNA expression quantified by quantitative PCR (qPCR; Figure 3b). In addition to these findings, EMT was observed in the *PIK3CA*-GEMM tumors. As shown in Figure 3c, in contrast to the universal expression of the epithelial marker E-cadherin (green) in control tumors, E-cadherin expression was lost in the *PIK3CA*-GEMM tumors. Conversely, the mesenchymal marker Vimentin (red) was expressed only in the stroma of the control tumors, but was expressed in the epithelium of *PIK3CA*-GEMM tumors, suggesting that EMT had taken place. This was further confirmed by qPCR showing decreased E-cadharin and increased Vimentin mRNA expression in the *PIK3CA*-GEMM tumors (Figure 3d). Last, relative to controls, the *PIK3CA*-GEMM tumors showed significantly increased expression of several transcription factors regulating EMT, including Twist1, Zeb1, Zeb2 and Snail1 (Figure 3e). Thus, the *PIK3CA*-GEMM tumors exhibited both histopathological and molecular signature of EMT.

It has been shown that de-differentiation and EMT correlate with enhanced CSC/progenitor activity.[20] We thus examined putative CSC markers of HNSCC by qPCR. As shown in Figure 3f, overexpression of *PIK3CA* significantly increased the mRNA expression of CD44 and CD166, and reduced the expression of CD24, all of which indicate an enhanced CSC phenotype. This result is further supported by increased mRNA expression of embronic stem cell markers Nanog, Oct4 and EZH2. Interestingly, increased expression of Wnt5a, which is implicated in migration/invasion, was also found in the *PIK3CA*-GEMM tumors (Figure 3f).

PIK3CA-GEMM tumors have increased PDK1 expression and activation

To investigate the molecular mechanisms of *PIK3CA*-driven HNSCC progression, we examined several key molecules in the PI3K pathway. It has been shown that the change of mRNA expression ratio between AKT1 and AKT2 regulates EMT in breast cancer cells.[21] However, there were no significant changes of mRNA expression of AKT1, AKT2, PDK1 or PTEN in the *PIK3CA*-GEMM tumors compared with control tumors (Figure 4a). AKT1 and AKT2 protein levels were similar between control and *PIK3CA*-GEMM tumors. However, PDK1 protein levels were increased in *PIK3CA*-GEMM tumors (Supplementary Figure 4). We then examined AKT and PDK1 protein activation by western blotting. Surprisingly, we did not detect significant differences in AKT phosphorylation at either Ser473 or Thr308 between the control and the *PIK3CA*-GEMM tumors. However, PDK1 activation by phosphorylation at Ser241 was significantly enhanced in *PIK3CA*-GEMM tumors (Figure 4b). Similarly, immunohistochemistry (IHC) staining showed an increase of total PDK1 protein in the *PIK3CA*-GEMM tumors (Figure 4c). These findings were unexpected and suggested that PDK1 may mediate oncogenic signaling in *PIK3CA*-driven HNSCC progression. Last, we examined several molecules that are commonly altered in human HNSCCs. 4NQO exposure causes the formation of DNA adducts, resulting in mutations.[19] We first examined two oncogenes that are commonly mutated in HNSCC, that is, *Ras* and *PIK3CA*. We sequenced eight *PIK3CA*-GEMM tumors and eight control tumors for mutations at codons 12, 13 and 61 of the *K-ras* and *H-ras* genes, and exons 9 and 20 of the *PIK3CA* gene. The only mutation we found was a G to A point mutation in codon 12 of mouse *K-ras* gene, which changes glutamic acid to aspartic acid (Supplementary Figure 5). This mutation was found only in one control tumor. We then examined the mRNA levels of *p16*, *EGFR*, *Stat3*, *CyclinD1*, *K-ras*, *H-ras* and *N-ras* in *PIK3CA*-GEMM and control tumors. We found increased *Stat3* and decreased *p16* mRNA in the *PIK3CA*-GEMM tumors compared with control tumors (Figure 4d).

To further examine whether PDK1 is involved in the tumor progression of the *PIK3CA*-GEMM mice, we cultured primary tumor cells from both *PIK3CA*-GEMM tumors (CU110 cells) and control tumors (CUCON cells). As shown in the Supplementary Figure 6A, consistent with the EMT changes in the tumor tissues, CU110 cells were more spindle-like, whereas CUCON cells were more round and epithelial-like. Overexpression of p110α was observed in the CU110 cells compared with that in CUCON cells (Figure 6e, left panel). We then stablely knocked down PDK1 in the CU110 cells (CU110-shPDK1), along with CU110 cells with a scramble insert (CU110-SCR) as a control (Figure 4e and Supplementary Figure 6B). Knocking down PDK1 in the CU110 cells increased E-cadherin expression and decreased Vimention expression (Figure 4e), but had no effects on phosphorylations of Smad2 or Smad3 (Supplementary Figure 6B). In addition, knocking down PDK1 (CU110-shPDK1) significantly reduced cell proliferation compared with the control cells (CU110-SCR; Figure 4f). Moreover, knocking down PDK1 in the CU110 cells moderately attenuated cell migration (Figure 4g) and invasion (Figure 4h) abilities. These data suggested that PDK1 contributed to the tumor progression phenotypes observed in the PIK3CA overexpression HNSCCs.

PIK3CA overexpression led to increased inflammation in HNSCC tumor stroma

In addition to the de-differentiation and EMT changes in the *PIK3CA*-GEMM tumor cells, we observed numerous infiltrated leukocytes in the stroma of the *PIK3CA*-GEMM tumors on histological sections examined by hematoxylin and eosin staining (Supplementary Figure 7) and IHC with CD45 (Figure 5a). We then examined subtypes of infiltrated leukocytes using IHC. Tumor-associated macrophages are stained by F4/80 antibody, and myeloid-derived suppressor cells in a tumor microenvironment are stained by granulocyte markers Gr1 and CD11b.[22] Both cell types were increased in *PIK3CA*-GEMM tumors compared with control tumors (Figure 5a). Last, we evaluated which cancer-associated inflammatory cytokines were upregulated in *PIK3CA*-GEMM tumors. Among the 15 inflammatory chemokines/receptors we evaluated, mRNA levels of CCL3, CCR7, CXCL12 and CXCR4 were all significantly increased in the *PIK3CA*-GEMM tumors compared with the control tumors (Figure 5b).

PIK3CA-GEMM tumors have increased TGFβ1 ligand, and increased Smad3 expression and activation

The EMT change in tumor cells and the enhanced leukocyte infiltration in *PIK3CA*-GEMM tumors are similar to what we observed previously in HNSCC mouse models with aberrant TGFβ signaling.[18,23,24] This prompted us to further investigate whether TGFβ signaling contributes to *PIK3CA*-driven HNSCC progression. We first used quantitative reverse transcription–PCR (qRT–PCR) to examine several TGFβ signaling pathway molecules known to be altered in human cancers. We found that mRNA levels of TGFβ1 and Smad3 were significantly higher in *PIK3CA*-GEMM tumor tissues than in control tumor tissues (Figure 6a). TGFβ1 protein level was also increased in the *PIK3CA*-GEMM tumor tissues, as determined by ELISA (Figure 6b). We then performed double IF of Smad3 and the epithelial marker E-cadherin. As shown in Figure 6c, the Smad3-positive area was inversely correlated with E-cadherin-positive staining, suggesting that Smad3 may contribute to the EMT changes in the *PIK3CA*-GEMM tumors. Increased phosphorylation of Smad3 in the *PIK3CA*-GEMM tumors compared with the control tumor tissues was also observed through western blot analysis (Figure 6d).

To further assess the role of TGFβ signaling in mediating the tumor-promoting effects of *PIK3CA* overexpression, we created CU110 cells in which the *PIK3CA* gene was knocked down

(CU110-shPIK3CA), along with CU110 cells with a scramble insert (CU110-SCR) as a control (Figure 6e, right panel). To examine the effect of *PIK3CA* overexpression or knockdown on TGFβ pathway in the cultured HNSCC cells to check whether *PIK3CA*-mediated regulation of TGFβ pathway is cell autonomous in cancer cells, we compared TGFβ1 mRNA levels in CUCON, CU110, CU110-*shPIK3CA* and CU110-*SCR* cells. As shown in Figure 6f, TGFβ mRNA levels in the CU110 cells were about four times than that in the CUCON cells. Conversely, knocking down *PIK3CA* significantly reduced TGFβ1 mRNA levels in CU110-*shPIK3CA* cells compared with the CU110-*SCR* cells, suggesting that the *PIK3CA*-mediated regulation of TGFβ pathway is cell autonomous in cancer cells. Last, we treated the *PIK3CA*-overexpressing CU110 cells with a TGFβ type I receptor kinase inhibitor, LY2157299, to address the contribution of TGFβ pathway to the *PIK3CA*-driven HNSCC progression. Treatment with LY2157288 effectively reduced Smad2 and Smad3 phosphorylation, indicating the effectiveness of the inhibition of the TGFβ signaling pathway (Figure 6g). Following the treatment,

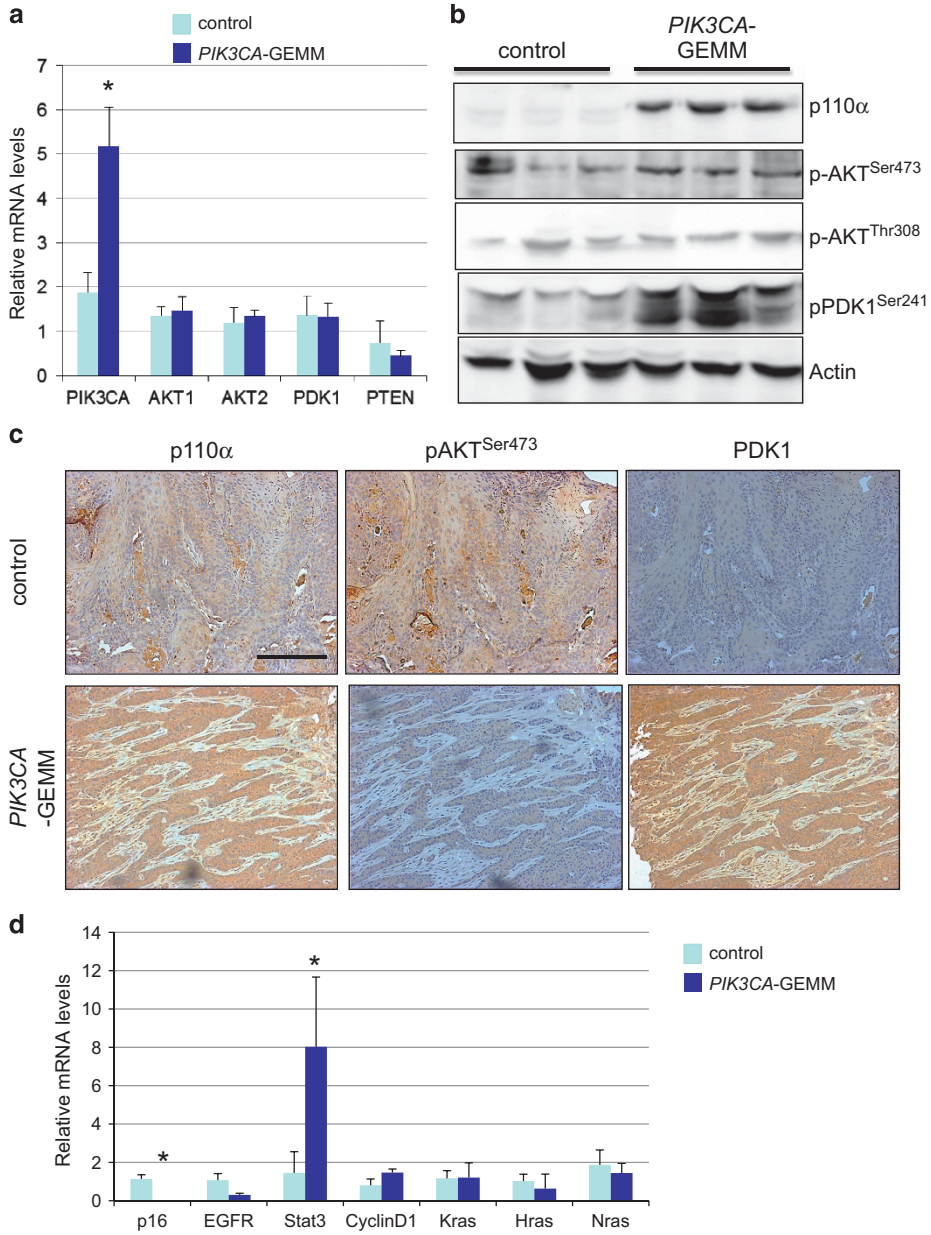

Figure 4. Overexpression and activation of PDK1 but not AKT in *PIK3CA*-GEMM tumors. (**a**) Relative mRNA levels of PIK3CA, AKT1, AKT2, PDK1 and PTEN measured by qRT–PCR. Results are averages of triplicate experiment. *$P < 0.05$ ($n = 6$ for each group). (**b**) Western blotting analysis of tumor samples from control mice and *PIK3CA*-GEMMs using the antibodies as indicated. (**c**) Immunohistochemistry (IHC) staining of p110α, pAKT^{ser473} and PDK1 in tumors from *PIK3CA*-GEMMs and control mice. Scale bar: 50 μM. (**d**) qRT–PCR examination of mRNA levels of molecules commonly altered in human HNSCCs. Results are averages of triplicate experiments. *$P < 0.05$ ($n = 6$ for each group). (**e**) Relative mRNA levels of PDK1, E-cadherin and Vimentin in CU110 cells with PDK1 knockdown (CU110-shPDK1) or with a scramble control (CU110-SCR) measured by qRT–PCR. *$P < 0.05$. (**f**) Cell proliferation assay of CU110-shPDK1 and CU110-SCR measured by the Cell Counting Kit-8. *$P < 0.05$. (**g**) Migration assay in CU110-shPDK1 and CU110-SCR cells. Dotted line defines the edges of cells. All experiments were performed in triplicate. *$P < 0.05$. (**h**) Invasion assay in CU110-shPDK1 and CU110-SCR cells. All experiments were performed in triplicate. *$P < 0.05$.

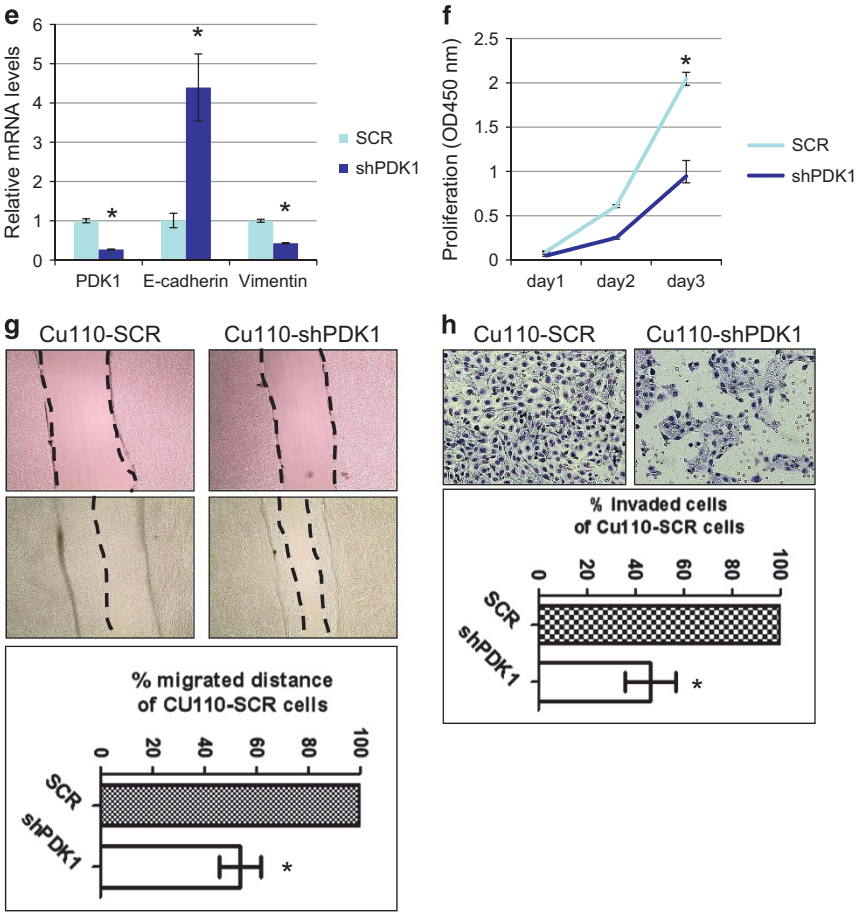

Figure 4. (Continued).

both cell migration and invasion were significantly hampered (Figures 6h and i), with a minor effect on cell proliferation (Supplementary Figure 6C), indicating that the TGFβ pathway contributes to migration and invasion of *PIK3CA*-driven HNSCC tumorigenesis.

PIK3CA and PDK1 are associated with progression in human HNSCC

To address the clinical relevance of our results from the *PIK3CA*-GEMM, we examined PIK3CA, PDK1 and pAKT expression levels in primary human HNSCC samples, case-matched adjacent mucosa and metastatic lesions, compared with normal oropharyngeal samples from patients with sleep apnea as controls. We first performed qRT–PCR to measure *PIK3CA* mRNA levels. Compared with normal controls, *PIK3CA* mRNA was increased in both adjacent mucosa and HNSCC samples (Figure 7a). Interestingly, increased *PIK3CA* expression positively correlated with reduced tumor differentiation and increased lymph node metastasis (Figure 7a). We then carried out IHC staining of p110α, PDK1 and pAKT. Figures 7b summarizes the percentage of cases with immunostaining $\geqslant 2+$ in HNSCC tumors and metastases. Consistent with *PIK3CA* qRT–PCR results, we found increased p110α immunostaining both in poorly differentiated HNSCCs and in metastases (Figures 7b and c). Interestingly, PDK1 expression positively correlated with *PIK3CA* expression and advanced disease (Figure 7b and c). However, AKT activation showed the opposite pattern, and demonstrated reduced expression in poorly differentiated tumors and metastases compared with early-stage lesions. These data from human tissue sample support our mouse model data that *PIK3CA*-driven HNSCC progression is predominantly mediated through PDK1, but not through AKT.

DISCUSSION

Previous mouse models were generated by knocking in *PIK3CA* mutant *H1047* into different tissue contexts.[25–29] However, somatic mutations of *PIK3CA* are infrequent (~10%) compared with *PIK3CA* gene amplification (~40%) in HNSCC patients.[4,5] Thus, our *PIK3CA*-GEMM, in which the wild-type *PIK3CA* is overexpressed specifically in murine head and neck epithelium, more closely mimics the majority of human HNSCC patients. As this transgene can be induced in a spatio-temporal manner, our model is an ideal platform to assess the role of *PIK3CA* overexpression at each stage of HNSCC tumorigenesis. This also represents the first GEMM in head and neck tissue for studying the *in vivo* role of *PIK3CA*.

In the *PIK3CA*-GEMM, we found that *PIK3CA* overexpression alone is not sufficient to initiate tumor formation in head and neck tissue. This is in contrast to the results of tumor formation in breast and lung cancer mouse models.[25–27] One explanation is that previous mouse models were based on gene mutations compared with our model, which is based on gene overexpression; these two types of gene alterations may play distinct roles in tumorigenesis. The other possibility is that *PIK3CA* may have a context-specific role in tumorigenesis. For example, the same mutant *PIK3CA-H1047* that causes spontaneous breast and lung tumor formation is not sufficient to initiate tumor formation in ovarian or colon tissues unless coupled with either a *PTEN* or *APC* deletion.[28,29] Our data suggest that *PIK3CA* overexpression may not initiate

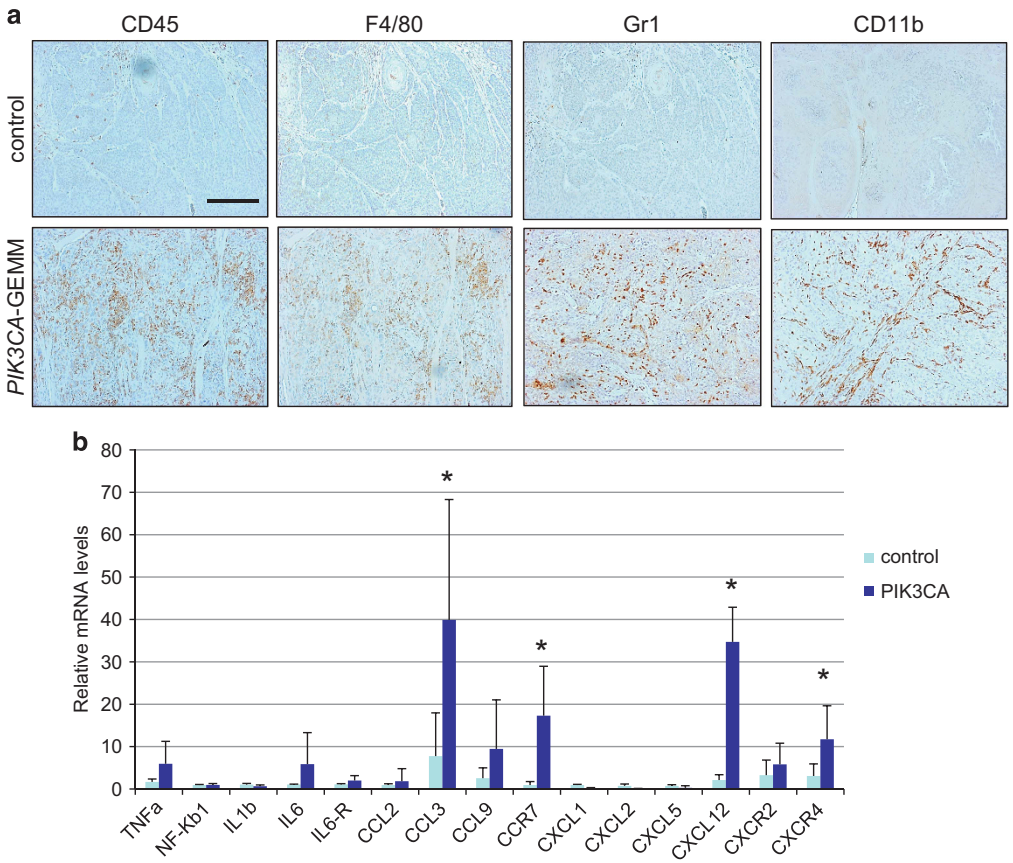

Figure 5. Increased leukocyte infiltration and inflammation in tumors from *PIK3CA*-GEMMs. (**a**) Detection of leukocyte subtypes in tumors from *PIK3CA*-GEMMs and control mice using IHC with CD45, F4/80, Gr1 and CD11b. Scale bar: 50 μm. (**b**) qRT–PCR examination of inflammatory-related cytokines/chemokines and receptors. Results are averages of triplicate experiments. $*P < 0.05$ ($n = 6$ for each group).

tumorigenesis, but instead it promotes tumor progression in HNSCC.

Compared with the well-documented mitogenic signaling of PI3K in cell growth and survival, the role of PI3K in tumor invasion and metastasis has not been well delineated. In a subset of aggressive breast cancer, which exhibits EMT and CSC characteristics, the authors found the mutation rate of *PIK3CA* reached nearly 50%, significantly higher than in any other types of breast cancer.[30] Knocking in the *PIK3CA* mutant into a breast cancer cell line also resulted in an EMT phenotype.[31] In line with these data, our *PIK3CA*-GEMM provides the first *in vivo* evidence that *PIK3CA* alteration is able to drive tumor progression at least partially through enriched EMT and CSC characteristics, which may be responsible for the invasive and metastatic phenotype observed in the *PIK3CA*-GEMM.

AKT is largely regarded as the dominant mediator of oncogenic PI3K signaling.[4] However, studies suggest that the link between PI3K and AKT can be uncoupled.[7,8,32,33] Recent reports showed that AKT can directly phosphorylate Twist1 to promote EMT,[34] and that the ratio of AKT1 and AKT2 and its regulated microRNAs are responsible for EMT and CSCs.[21] However, we found no differences in AKT activation or expression of AKT isoforms between control and *PIK3CA*-GEMM tumors. Lack of AKT activation has also been observed in subset of *PIK3CA*-mutated breast cancer,[8] *PTEN*-null lung cancers[35] and *BRAF*-initiated melanoma.[9] AKT activation can be detected in mouse models as early as pre-neoplastic lesions upon either 4NQO[36] or NNK treatment,[37] and AKT activation in the oral cavity can initiate benign tumor formation. However, it fails to promote tumor progression unless combined with *p53* loss,[38] suggesting that AKT activation may be involved in early events in HNSCC carcinogenesis, but not in tumor progression. In some breast cancers with *PIK3CA* mutations, PDK1, but not AKT, is activated.[8] Similarly, our results suggest that PDK1, rather than AKT, facilitates progression of PI3K-driven HNSCC, which raises the possibility of PDK1 as a therapeutic target in HNSCC patients with *PIK3CA* alterations.

PDK1 is a serine/threonine protein kinase that phosphorylates members of the AGC kinase superfamily, including AKT, and is implicated in cell proliferation, survival and metabolism.[39] Interestingly, PDK1 has been shown to regulate cell migration but not proliferation in lymphocytes,[40] and to promote EMT in cardiac development.[41] Compared with the extensive research into AKT, less is known about the role of PDK1 in human cancers. Overexpression of PDK1 has been reported in several human cancers,[42–44] and correlates with disease progression in patients with pancreatic cancer or melanoma.[43,44] Interestingly, PDK1 is required for *Kras*-driven pancreatic cancer in murine models but not for the *Kras*-driven lung cancer, suggesting a context-specific role of PDK1.[45] In HNSCC, PDK1 has been shown to mediate G-protein-coupled receptor and epidermal growth factor receptor (EGFR) cross-talk as well as cell growth, both *in vitro* and *in vivo*.[46] It has become evident recently that the role of PDK1 in physiological and pathological conditions is not limited to AKT activation; it may also evoke other signaling for tumorigenesis. For example, PDK1 has been shown to activate SGK3 in a PI3K-dependent, AKT-independent manner in breast cancer.[8] PDK1 can also directly activate PLCγ1 to mediate cancer cell invasion.[47] Moreover, PDK1 directly phosphorylates polo-like kinase 1 to induce an embryonic stem cell-like gene signature associated with aggressive tumor behaviors and CSC self-renewal.[48] Further investigation on the

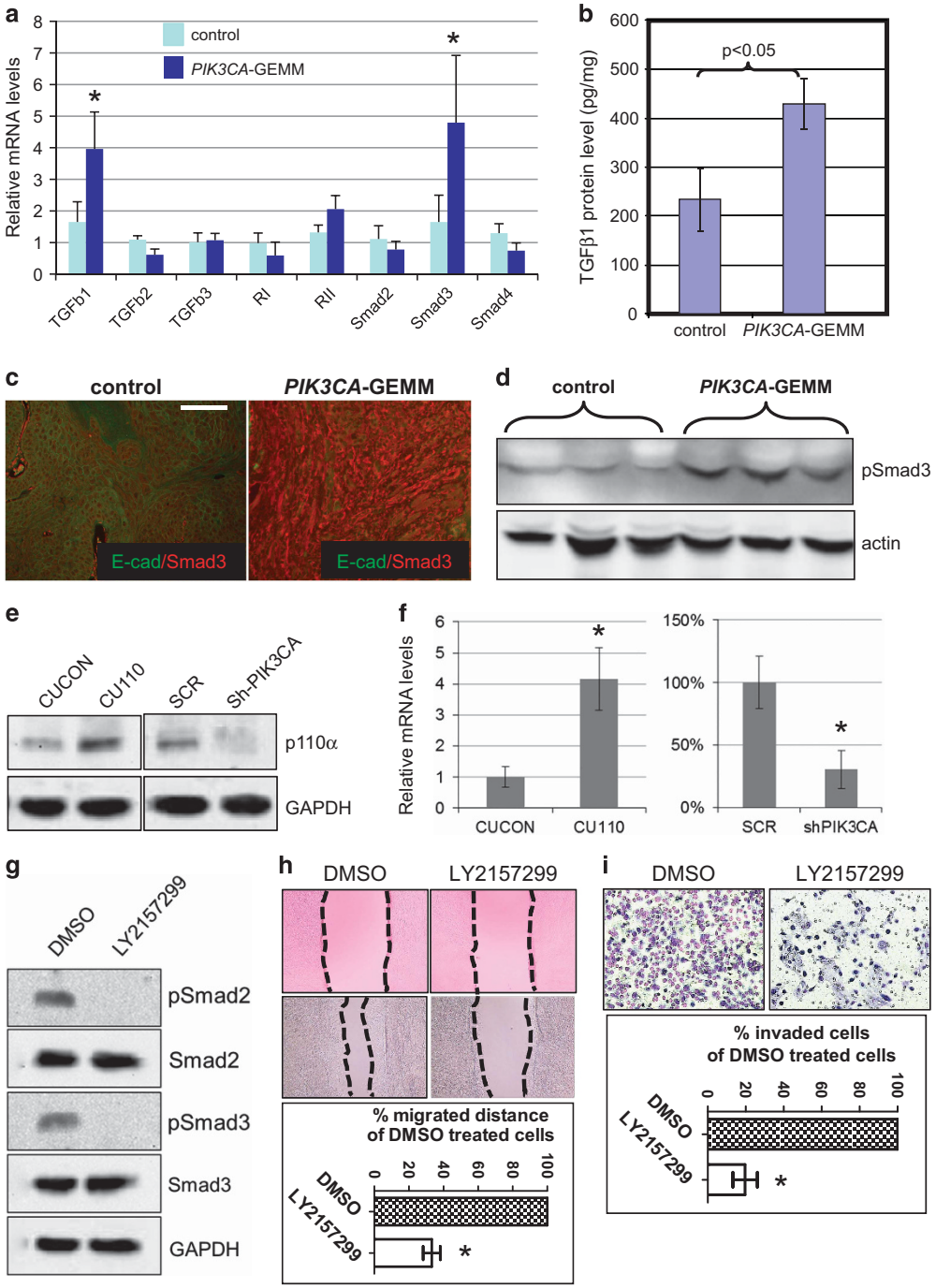

Figure 6. Increased TGFβ ligand and smad3 expression and activation in tumors from *PIK3CA*-GEMMs. (**a**) qRT–PCR examination of molecules in the TGFβ signaling pathway. *$P < 0.05$ ($n = 6$ for each group). (**b**) ELISA quantification of TGFβ1 ligand ($n = 5$). (**c**) Double IF staining of epithelial marker E-cadherin (green) and Smad3 (red). Note the inverse correlation between Smad3 and E-cadherin in control and *PIK3CA*-GEMM tumors. ($n = 4$), scale bar: 25 μm. (**d**) Western blot analysis of phosphorylated Smad3. (**e**) Western blot analysis of p110α in cells cultured from a 4NQO-induced control tumor (CUCON) and a 4NQO-induced *PIK3CA*-GEMM tumor (CU110), and CU110 cells with either a *PIK3CA* knockdown (*shPIK3CA*) or a scramble control (*SCR*). (**f**) qRT–PCR examination of TGFβ1 mRNA levels in CUCON and CU110 cells (left panel), and CU110 cells with *PIK3CA* knockdown (*shPIK3CA*) or scramble control (*SCR*; right panel). *$P < 0.05$. (**g**) Western blot analysis of phosphorylation of Smad2 and Smad3 in CU110 cells treated with a TGFβ type I receptor inhibitor, LY2157299, or dimethyl sulfoxide (DMSO; control). (**h**) Migration assay in CU110 cells treated with a TGFβ type I receptor inhibitor, LY2157299, or DMSO (control). Dotted line defines the edges of cells. All experiments were performed in triplicate. *$P < 0.05$. (**i**) Invasion assay in CU110 cells treated with a TGFβ type I receptor inhibitor, LY2157299, or DMSO (control). All experiments were performed in triplicate. *$P < 0.05$.

downstream molecular mechanisms underlying PI3K/PDK1 signaling in the *PIK3CA*-GEMM will provide important insights into *PIK3CA*-driven HNSCC progression and identify novel therapeutic targets to control HNSCC progression.

The downstream mechanisms of PI3K/PDK1 in HNSCC invasion and metastasis are largely unknown. In this study, we found that the TGFβ1 ligand and its downstream mediator Smad3 are overexpressed in *PIK3CA*-GEMM tumor tissues. The positive

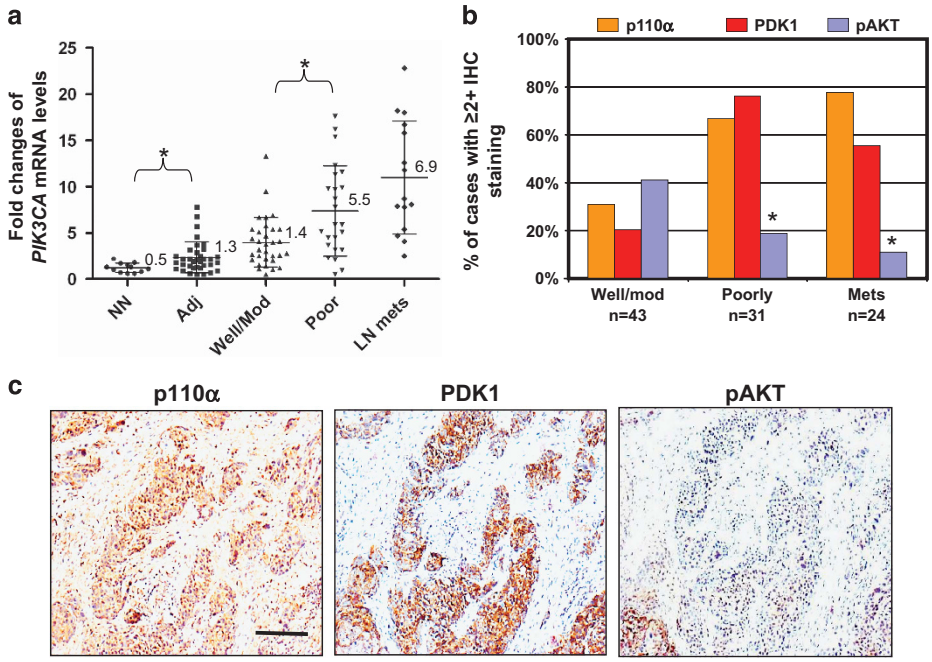

Figure 7. PIK3CA, PDK1 and pAKT alterations in human HNSCCs. (**a**) qRT–PCR quantitation of *PIK3CA* mRNA expression in human HNSCCs. Error bars indicate mean ± s.d. *$P < 0.05$. Adj, adjacent mucosa; LN mets, lymph node metastases; Mod, moderately differentiated tumors; NN, normal controls; Poorly, poorly differentiated tumors; Well, well-differentiated tumors. (**b**) Percentage of human HNSCC cases which exhibited ⩾ 2+ IHC staining of p110α, PDK1 and pAKT. *$P < 0.05$. (**c**) IHC staining of serial sections of a poorly differentiated HNSCC. Scale bar: 50 μm.

correlation between *PIK3CA* and TGFβ1 levels was further detected in both PIK3CA-overexpressing tumor cells and *PIK3CA*-knockdown tumor cells, suggesting that the *PIK3CA*-mediated regulation of TGFβ pathway is cell autonomous. The contribution of TGFβ pathway to mediate migration and invasion of *PIK3CA*-overexpressing tumor cells was validated by treating these cells with a TGFβ pathway inhibitor. Cross talk between PI3K and TGFβ signaling can occur at multiple levels.[49] For example, PI3K is able to mediate TGFβ-receptor-initiated intracellular signaling.[50] In addition, PI3K can antagonize TGF-β-induced cytostasis and cause the shift in TGFβ signaling to tumor progression.[49] However, prior reports on PI3K and TGFβ interplay were almost exclusively related to AKT signaling.[49] Thus, it remains unclear how PI3K/PDK1 interacts with TGFβ/Smad3 signaling during HNSCC progression.

Currently, the only Food and Drug Administration-approved targeted therapy for HNSCC is EGFR inhibitors.[51] Targeting the PI3K pathway represents a promising new strategy for treating HNSCC. The role of PDK1 in mediating invasion and metastasis of *PIK3CA*-driven HNSCC suggests it may be useful as a therapeutic target. Targeting PDK1 using either genetic approaches or pharmaceutical inhibitors has been shown to inhibit CSC self-renewal and metastasis.[44,48,52] In one pre-clinical study on HNSCC, PDK1 inhibition showed anti-tumor effects either by itself or in combination with EGFR inhibition.[46] Thus, targeting PIK3CA or PDK1 presents an important new avenue for HNSCC treatment. Targeting TGFβ as anti-cancer therapy has been evaluated for a decade in multiple cancers.[53] However, it remains unclear how it may best be used and such therapies are highly stage- and patient-specific. The possible synergistic role of overactivated PI3K and TGFβ signaling in HNSCC progression demonstrated in this study has prompted testing of combination therapy. If proven effective in pre-clinical trials with *PIK3CA*-GEMM, this combination therapy will be immediately translated into clinical trials for treating advanced HNSCC patients who have *PIK3CA* alterations.

In summary, we report a GEMM in which the *PIK3CA* is overexpressed in head and neck epithelia. Although overexpression of *PIK3CA* alone is not sufficient to initiate HNSCC formation, it significantly increased the susceptibility to the 4NQO-induced HNSCC carcinogenesis. More importantly, *PIK3CA* overexpression promotes EMT and CSC properties and drives tumor invasion and metastasis, which is likely mediated by increased PDK1 expression and activation, and subsequently increased TGFβ1 ligand and Smad3 expression and activation. Our study lays the foundation for future investigations into the mechanism of PDK1 and its interplay with TGFβ signaling in *PIK3CA*-driven HNSCC tumorigenesis. Moreover, it suggests that therapeutic targeting of PDK1 and/or TGFβ signaling may effectively control HNSCC progression, particularly in patients with *PIK3CA* amplification.

MATERIALS AND METHODS

Generation and characterization of the inducible head-and-neck-specific PIK3CA GEMM

All animal experiments were performed in accordance with protocols approved by the Institutional Animal Cancer and Use Committees of the Oregon Health and Science University (OHSU) and University of Colorado School of Medicine. The plasmid containing full-length cDNA of *PIK3CA* (*pcDNA3.1-PIK3CA*) was obtained from Addgene (Cambridge, MA, USA) under the material transfer agreement agreement. The *PIK3CA* fragment was subcloned into the target vector (ptata.A) using the *Xho*I site (Supplementary Figure 8a). A 3.5-kb *Hin*dIII/*Kpn*I fragment including Gal4-binding sites, minimal tata promoter and the *PIK3CA* cDNA was microinjected into the pronucleus of single-cell embryo by the transgenic mouse core facility at OHSU. The embryos were implanted into pseudo-pregnant females and allowed to develop to term. PCR genotyping was performed at the 3 weeks of age using genomic DNA isolated from tail biopsies. Three lines (#5840, #5446, #5703) transmitted the transgene through their germline and was called *tata.PIK3CA* mouse line thereafter (Supplementary Figure 8b). The transgene-specific primers covering hemagglutinin tag were designed, along the upstream sequence. The primers used to detect the *ptata.PIK3CA* transgene were: forward: 5′-TGAGCAAGAGGCTTTGGAGT-3′ and reverse: 5′-TGCATTCTAGT TGTGGTTT-3′.

The target mouse line *tata.PIK3CA* was then bred to the trans-activator mouse line, *K5.GLp65*, which was developed previously.[18] The resulting bigenic mouse line *K5.GLp65/tata.PIK3CA* is hereafter referred to as *PIK3CA*-GEMM. The *PIK3CA*-GEMMs were selected by using genotyping primers specific for GLp65 (forward: 5′-TGTCAAGGTCTTCTCGAGGA-3′;

reverse: 5′-GGCCATACACTTGAGTGACA-3′), and the same primers that were used for detection of the *PIK3CA* transgene (above).

All mouse experiments were performed in a C57BL/6 background. Adult bigenic *K5.GLp65/tata.PIK3CA* and monogenic *K5.GLp65*, *tata.PIK3CA* and non-transgenic mice (around 1-month-old) were treated with RU486 for *PIK3CA* gene induction and with the rodent oral carcinogen, 4NQO (Sigma, St Louis, MO, USA). For the transgene induction, 100 µl of RU486, dissolved in sesame oil (0.2 µg/ml), was applied in the oral cavity of mouse to induce either acute or sustained *PIK3CA* transgene expression as described previously.[18] For the oral carcinogenesis experiment, 4NQO (Sigma) was prepared weekly in propylene glycol at a concentration of 5 mg/ml, and was placed into drinking water in a final concentration of 50 µg/ml. The water was changed once weekly, and was given to mice for 16 weeks. The general health condition of mice was monitored twice weekly, and their body weight was measured once weekly. Mice were given softened food when there were signs of food-intake difficulty, or decreased body weight. At the end of animal experiment, mice were euthanized. Buccal mucosa, tongue, lymph node and lung tissues were harvested for histological analysis and immunostaining.

Patients

The clinical study protocol was approved by the Institutional Review Board-approved of OHSU, and written informed consent was obtained from all participants before sample collection. HNSCC and case-matched adjacent tissue samples were surgically resected from consenting patients at the Departments of Otolaryngology and Dermatology of OHSU. Tissues examined in this study include a total of 74 HNSCCs (26 SCCs of tongue, 19 SCCs of oral cavity, 3 SCCs of nasal pharynx, 7 SCCs of oropharynx, 7 SCCs of hypopharynx, 12 SCCs of larynx) and case-matched tissues adjacent to tumors, and 24 cases of lymph node metastases. A total of 12 normal oropharyngeal samples from sleep apnea patients were used as normal controls.

Histology and immunostaining

Tissues were fixed in 10% neutral buffered formalin, embedded in paraffin and sectioned to 5-µm thickness. Sections were stained with hematoxylin and eosin and examined for the presence of hyperplasia, dysplasia, papillomas, carcinomas and metastases. Tumor pathology and metastasis were examined by at least two investigators and confirmed by the head and neck cancer pathologist (SS). Quantitation of IHC staining of human p110α, pAKT and PDK1 was performed by two independent investigators using methods described previously.[54] Double immunofluorescence was performed as previously described.[24] Incubation with primary antibodies was as follows: Keratin 1 (K1; Convance Princeton, NJ, USA, PRB-165 P), K8 (Fitzgerald, Acton, MA, USA, 20 R-CP004), Ecadherin (Cell Signaling, Danvers, MA, USA, #3195), Vimentin (BD Pharmingen, San Jose, CA, USA, RV202), Smad3 (Novus, Littleton, CO, USA, 378611). Immunohistochemistry was performed as described previously.[24] Incubation with primary antibodies was as followings: PDK1 (Abcam, Cambridge, MA, USA, ab52893), CD45 (eBioscience, San Diego, CA, USA, 14-0451), F4/80 (Serotec, Raleigh, NC, USA, MCA497GA), Gr1 (BD Pharmingen, 550291), CD11b (BD Pharmingen, 550282), p110α (Cell Signaling, #4249), Ki67 (Abcam, ab16667) and pAKT^{Ser473} (Cell Signaling, #3787). Slides were examined with a Leica microscope, and images were taken using the Q Capture Pro software (Q imaging, Surrey, BC, USA).

DNA sequencing, RNA isolation and qRT–PCR

Genomic DNA isolation from mouse tumor tissues was performed as described previously.[23] Exon 1 and exon 2 of mouse *H-ras*, or *K-ras*, and exon 9 and exon 20 of mouse *PIK3CA* were amplified by PCR and sequenced using the sequences listed in Supplementary Table 1. RNA isolation and cDNA synthesis were performed as described previously.[24] cDNAs were subjected to qRT–PCR using either the SYBR mix (Bio-Rad, Hercules, CA, USA) or the TaqMan Assays-on-Demand probes (Applied Biosystems, Foster City, CA, USA). qRT–PCR was run on the CFX connect qPCR machine (Bio-Rad). β-Actin was used as an internal control. Primer sequences for mouse SYBR qRT–PCR assay are listed in Supplementary Table 2. Primer sequences for human *PIK3CA* qRT–PCR are: forward-5′-ACC TGAATAGGCAAGTCGAGGCAA-3′, reverse-5′-ACAGAAAGCCCTGTAGAGCAT CCA-3′. Each sample was examined in triplicate. The relative RNA expression levels were determined by normalizing to the internal control, the values of which were calculated using the comparative Ct method.

Protein analysis

Whole head and neck tissues and tumors tissues were lysed using a homogenizer (Pro Scientific, Oxford, CT, USA) in lysis buffer (Roche, Indianapolis, IN, USA) containing a pellet of protease inhibitor cocktail. Protein concentration was measured using Pierce 660 nm protein assay reagent (Thermo, Waltham, MA, USA), and 40 µg of protein lysates were analyzed using the standard western blot protocol we have described previously.[37] Blots were incubated with primary antibodies at 4 °C overnight and secondary antibodies for 1 h at room temperature. Western blots were imaged by ECL (Bio-Rad) and normalized with respect to GAPDH (Cell Signaling, #5174) expression. The primary antibodies were used as follows and purchased from Cell Signaling: p110α (#4255), PDK1 (#3438), pPDK1^{Ser241} (#3061), pAKT^{Ser473} (#4058), pAKT^{Thr308} (#9275), AKT1 (#2938), AKT2 (#4057), pSmad2$^{ser465/467}$ (#3101) and pSmad3$^{ser423/425}$ (#9520). TGFβ1 ELISA was performed as described previously using the R&D Systems kit (R&D Systems, Minneapolis, MN, USA).[18]

Cell culture

Cells were cultured from either a 4NQO-induced control tongue SCC (CUCON) or a 4NQO-induced *PIK3CA*-GEMM tongue SCC (CU110). Tumor tissues were minced with blade, and digested in 0.35% collagenase (Gibco, Carlsbad, CA, USA) followed by two rounds of 1% trypsin digestion at 37 °C. Single cells were obtained through a cell strainer (70 mm nylon, BD Biosciences, Franklin lakes, NJ, USA), and plated at 1×10^5/ml in 10 cm dishes. Cells were cultured in DMEM+10% FBS and 100 U/ml penicillin/streptomycin (Gibco). The authentication of the cultured cells was validated by the transgene-specific genotyping PCR (Supplementary Figure 2).

Knockdown experiment. PIK3CA or PDK1 knockdown was achieved using a lentiviral-based shPIK3CA or shPDK1 purchased from Sigma (MISSION shRNA). TRCN0000361413 or TRCN0000361331 was used for mouse PIK3CA or PDK1 Knockdown, respectively, and SHC002 as a scramble control.

Cell Proliferation assay. Cells were seeded into 24-well plates as 1×10^5 cells/well, and were treated with 0–80 µM LY2157299 (MedKoo Biosciences, Chapel hill, NC, USA) for 48 h. The cell proliferation was determined by using Vi-cell XR cell viability analyzer (Beckman Coulter, Brea, CA, USA). For the cell proliferation assay in CU110-shPDK1 and CU110-SCR cells, the assay was performed using cell counting kit 8 (Dojindo Molecular Technologies, Rockville, MD, USA).

Migration and Invasion assay. The migration and invasion assays were performed using CytoSelect 24-well wound healing assay kit (Cell Biolabs, San Diego, CA, USA) and QCM ECMatrix cell invasion assay kit (EMD Millipore, Billerica, MA, USA). Three individual experiments were performed for each assay.

Statistical analysis

Statistical analysis for all qPCR data was performed using a two-sample equal variance and two-tailed Student's *t*-test. All of the above statistical analyses were performed using Prism4 (GraphPad, La Jolla, CA, USA). A *P*-value of less than 0.05 is considered statistically significant.

CONFLICT OF INTEREST

The authors declare no conflict of interest.

ACKNOWLEDGEMENTS

This work is supported by National Institutes of Health grant R01DE021788 (to S-L Lu), R01DE015953 (to X-J Wang). University of Colorado Academic Enrichment Fund (to S-L Lu), American Cancer Society (to S-L Lu), University of Colorado Cancer Center (to S-L Lu), and Cancer League of Colorado (to S-L Lu). S-L Lu is an investigator of THANC foundation. We thank the Transgenic Core of Oregon Health and Science University for generating founders of the mouse model, and the University of Colorado Skin Disease Research Center Morphology Phenotyping Core (P30 AR057212) for assisting with histological work.

REFERENCES

1 Jemal A, Bray F, Center MM, Ferlay J, Ward E, Forman D. Global cancer statistics. *CA Cancer J Clin* 2011; **61**: 69–90.
2 Siegel R, Naishadham D, Jemal A. Cancer statistics, 2013. *CA Cancer J Clin* 2013; **63**: 11–30.

3 Leemans CR, Braakhuis BJ, Brakenhoff RH. The molecular biology of head and neck cancer. *Nat Rev Cancer* 2011; **11**: 9–22.
4 Engelman JA, Luo J, Cantley LC. The evolution of phosphatidylinositol 3-kinases as regulators of growth and metabolism. *Nat Rev Genet* 2006; **7**: 606–619.
5 Liu P, Cheng H, Roberts TM, Zhao JJ. Targeting the phosphoinositide 3-kinase pathway in cancer. *Nat Rev Drug Discov* 2009; **8**: 627–644.
6 Du L, Shen J, Weems A, Lu SL. Role of phosphatidylinositol-3-kinase pathway in head and neck squamous cell carcinoma. *J Oncol* 2012; **2012**: 450179.
7 Vogt PK, Gymnopoulos M, Hart JR. PI 3-kinase and cancer: changing accents. *Curr Opin Genet Dev* 2009; **19**: 12–17.
8 Vasudevan KM, Barbie DA, Davies MA, Rabinovsky R, McNear CJ, Kim JJ *et al.* AKT-independent signaling downstream of oncogenic PIK3CA mutations in human cancer. *Cancer Cell* 2009; **16**: 21–32.
9 Marsh Durban V, Deuker MM, Bosenberg MW, Phillips W, McMahon M. Differential AKT dependency displayed by mouse models of BRAFV600E-initiated melanoma. *J Clin Invest* 2013; **123**: 5104–5118.
10 Lui VW, Hedberg ML, Li H, Vangara BS, Pendleton K, Zeng Y *et al.* Frequent mutation of the PI3K pathway in head and neck cancer defines predictive biomarkers. *Cancer Discov* 2013; **3**: 761–769.
11 Pickering CR, Zhang J, Yoo SY, Bengtsson L, Moorthy S, Neskey DM *et al.* Integrative genomic characterization of oral squamous cell carcinoma identifies frequent somatic drivers. *Cancer Discov* 2013; **3**: 770–781.
12 Iglesias-Bartolome R, Martin D, Gutkind JS. Exploiting the head and neck cancer oncogenome: widespread PI3K-mTOR pathway alterations and novel molecular targets. *Cancer Discov* 2013; **3**: 722–725.
13 Morris LG, Taylor BS, Bivona TG, Gong Y, Eng S, Brennan CW *et al.* Genomic dissection of the epidermal growth factor receptor (EGFR)/PI3K pathway reveals frequent deletion of the EGFR phosphatase PTPRS in head and neck cancers. *Proc Natl Acad Sci U S A* 2011; **108**: 19024–19029.
14 Woenckhaus J, Steger K, Werner E, Fenic I, Gamerdinger U, Dreyer T *et al.* Genomic gain of PIK3CA and increased expression of p110alpha are associated with progression of dysplasia into invasive squamous cell carcinoma. *J Pathol* 2002; **198**: 335–342.
15 Kozaki K, Imoto I, Pimkhaokham A, Hasegawa S, Tsuda H, Omura K *et al.* PIK3CA mutation is an oncogenic aberration at advanced stages of oral squamous cell carcinoma. *Cancer Sci* 2006; **97**: 1351–1358.
16 Estilo CL, O-Charoenrat P, Ngai I, Patel SG, Reddy PG, Dao S *et al.* The role of novel oncogenes squamous cell carcinoma-related oncogene and phosphatidylinositol 3-kinase p110alpha in squamous cell carcinoma of the oral tongue. *Clin Cancer Res* 2003; **9**: 2300–2306.
17 Fenic I, Steger K, Gruber C, Arens C, Woenckhaus J. Analysis of PIK3CA and Akt/protein kinase B in head and neck squamous cell carcinoma. *Oncol Rep* 2007; **18**: 253–259.
18 Lu SL, Reh D, Li AG, Woods J, Corless CL, Kulesz-Martin M *et al.* Overexpression of transforming growth factor beta1 in head and neck epithelia results in inflammation, angiogenesis, and epithelial hyperproliferation. *Cancer Res* 2004; **64**: 4405–4410.
19 Vitale-Cross L, Czerninski R, Amornphimoltham P, Patel V, Molinolo AA, Gutkind JS. Chemical carcinogenesis models for evaluating molecular-targeted prevention and treatment of oral cancer. *Cancer Prev Res (Phila)* 2009; **2**: 419–422.
20 Mani SA, Guo W, Liao MJ, Eaton EN, Ayyanan A, Zhou AY *et al.* The epithelial-mesenchymal transition generates cells with properties of stem cells. *Cell* 2008; **133**: 704–715.
21 Iliopoulos D, Polytarchou C, Hatziapostolou M, Kottakis F, Maroulakou IG, Struhl K *et al.* MicroRNAs differentially regulated by Akt isoforms control EMT and stem cell renewal in cancer cells. *Sci Signal* 2009; **2**: ra62.
22 Marvel D, Gabrilovich DI. Myeloid-derived suppressor cells in the tumor microenvironment: expect the unexpected. *J Clin Invest* 2015; **125**: 3356–3364.
23 Lu SL, Herrington H, Reh D, Weber S, Bornstein S, Wang D *et al.* Loss of transforming growth factor-beta type II receptor promotes metastatic head-and-neck squamous cell carcinoma. *Genes Dev* 2006; **20**: 1331–1342.
24 Bornstein S, White R, Malkoski S, Oka M, Han G, Cleaver T *et al.* Smad4 loss in mice causes spontaneous head and neck cancer with increased genomic instability and inflammation. *J Clin Invest* 2009; **119**: 3408–3419.
25 Liu P, Cheng H, Santiago S, Raeder M, Zhang F, Isabella A *et al.* Oncogenic PIK3CA-driven mammary tumors frequently recur via PI3K pathway-dependent and PI3K pathway-independent mechanisms. *Nat Med* 2011; **17**: 1116–1120.
26 Klarenbeek S, van Miltenburg MH, Jonkers J. Genetically engineered mouse models of PI3K signaling in breast cancer. *Mol Oncol* 2013; **7**: 146–164.
27 Engelman JA, Chen L, Tan X, Crosby K, Guimaraes AR, Upadhyay R *et al.* Effective use of PI3K and MEK inhibitors to treat mutant Kras G12D and PIK3CA H1047R murine lung cancers. *Nat Med* 2008; **14**: 1351–1356.
28 Kinross KM, Montgomery KG, Kleinschmidt M, Waring P, Ivetac I, Tikoo A *et al.* An activating Pik3ca mutation coupled with Pten loss is sufficient to initiate ovarian tumorigenesis in mice. *J Clin Invest* 2012; **122**: 553–557.
29 Hare LM, Phesse TJ, Waring PM, Montgomery KG, Kinross KM, Mills K *et al.* Physiological expression of the PI3K-activating mutation Pik3ca(H1047R) combines with Apc loss to promote development of invasive intestinal adenocarcinomas in mice. *Biochem J* 2014; **458**: 251–258.
30 Hennessy BT, Gonzalez-Angulo AM, Stemke-Hale K, Gilcrease MZ, Krishnamurthy S, Lee JS *et al.* Characterization of a naturally occurring breast cancer subset enriched in epithelial-to-mesenchymal transition and stem cell characteristics. *Cancer Res* 2009; **69**: 4116–4124.
31 Wallin JJ, Guan J, Edgar KA, Zhou W, Francis R, Torres AC *et al.* Active PI3K pathway causes an invasive phenotype which can be reversed or promoted by blocking the pathway at divergent nodes. *PLoS One* 2012; **7**: e36402.
32 Fan QW, Cheng C, Knight ZA, Haas-Kogan D, Stokoe D, James CD *et al.* EGFR signals to mTOR through PKC and independently of Akt in glioma. *Sci Signal* 2009; **2**: ra4.
33 Lauring J, Cosgrove DP, Fontana S, Gustin JP, Konishi H, Abukhdeir AM *et al.* Knock in of the AKT1 E17K mutation in human breast epithelial cells does not recapitulate oncogenic PIK3CA mutations. *Oncogene* 2010; **29**: 2337–2345.
34 Xue G, Restuccia DF, Lan Q, Hynx D, Dirnhofer S, Hess D *et al.* Akt/PKB-mediated phosphorylation of Twist1 promotes tumor metastasis via mediating cross-talk between PI3K/Akt and TGF-beta signaling axes. *Cancer Discov* 2012; **2**: 248–259.
35 Curry NL, Mino-Kenudson M, Oliver TG, Yilmaz OH, Yilmaz VO, Moon JY *et al.* Pten-null tumors cohabiting the same lung display differential AKT activation and sensitivity to dietary restriction. *Cancer Discov* 2013; **3**: 908–921.
36 Wong KK. Oral-specific chemical carcinogenesis in mice: an exciting model for cancer prevention and therapy. *Cancer Prev Res (Phila)* 2009; **2**: 10–13.
37 Weber SM, Bornstein S, Li Y, Malkoski SP, Wang D, Rustgi AK *et al.* Tobacco-specific carcinogen nitrosamine 4-(methylnitrosamino)-1-(3-pyridyl)-1-butanone induces AKT activation in head and neck epithelia. *Int J Oncol* 2011; **39**: 1193–1198.
38 Moral M, Segrelles C, Lara MF, Martínez-Cruz AB, Lorz C, Santos M *et al.* Akt activation synergizes with Trp53 loss in oral epithelium to produce a novel mouse model for head and neck squamous cell carcinoma. *Cancer Res* 2009; **69**: 1099–1108.
39 Pearce LR, Komander D, Alessi DR. The nuts and bolts of AGC protein kinases. *Nat Rev Mol Cell Biol* 2010; **11**: 9–22.
40 Finlay DK, Sinclair LV, Feijoo C, Waugh CM, Hagenbeek TJ, Spits H *et al.* Phosphoinositide-dependent kinase 1 controls migration and malignant transformation but not cell growth and proliferation in PTEN-null lymphocytes. *J Exp Med* 2009; **206**: 2441–2454.
41 Feng Q, Di R, Tao F, Chang Z, Lu S, Fan W *et al.* PDK1 regulates vascular remodeling and promotes epithelial-mesenchymal transition in cardiac development. *Mol Cell Biol* 2010; **30**: 3711–3721.
42 Maurer M, Su T, Saal LH, Koujak S, Hopkins BD, Barkley CR *et al.* 3-Phosphoinositide-dependent kinase 1 potentiates upstream lesions on the phosphatidylinositol 3-kinase pathway in breast carcinoma. *Cancer Res* 2009; **69**: 6299–6306.
43 Garcia-Carracedo D, Turk AT, Fine SA, Akhavan N, Tweel BC, Parsons R *et al.* Loss of PTEN expression is associated with poor prognosis in patients with intraductal papillary mucinous neoplasms of the pancreas. *Clin Cancer Res* 2013; **19**: 6830–6841.
44 Scortegagna M, Ruller C, Feng Y, Lazova R, Kluger H, Li JL *et al.* Genetic inactivation or pharmacological inhibition of Pdk1 delays development and inhibits metastasis of Braf::Pten melanoma. *Oncogene* 2013; **33**: 4330–4339.
45 Eser S, Reiff N, Messer M, Seidler B, Gottschalk K, Dobler M *et al.* Selective requirement of PI3K/PDK1 signaling for Kras oncogene-driven pancreatic cell plasticity and cancer. *Cancer Cell* 2013; **23**: 406–420.
46 Bhola NE, Freilino ML, Joyce SC, Sen M, Thomas SM, Sahu A *et al.* Antitumor mechanisms of targeting the PDK1 pathway in head and neck cancer. *Mol Cancer Ther* 2012; **11**: 1236–1246.
47 Raimondi C, Chikh A, Wheeler AP, Maffucci T, Falasca M. A novel regulatory mechanism links PLCgamma1 to PDK1. *J Cell Sci* 2012; **125**: 3153–3163.
48 Tan J, Li Z, Lee PL, Guan P, Aau MY, Lee ST *et al.* PDK1 signaling toward PLK1-MYC activation confers oncogenic transformation, tumor-initiating cell activation, and resistance to mTOR-targeted therapy. *Cancer Discov* 2013; **3**: 1156–1171.
49 Zhang L, Zhou F, ten Dijke P. Signaling interplay between transforming growth factor-beta receptor and PI3K/AKT pathways in cancer. *Trends Biochem Sci* 2013; **38**: 612–620.
50 Yi JY, Shin I, Arteaga CL. Type I transforming growth factor beta receptor binds to and activates phosphatidylinositol 3-kinase. *J Biol Chem* 2005; **280**: 10870–10876.
51 Du Y, Peyser ND, Grandis JR. Integration of molecular targeted therapy with radiation in head and neck cancer. *Pharmacol Ther* 2014; **142**: 88–98.
52 Signore M, Pelacchi F, di Martino S, Runci D, Biffoni M, Giannetti S *et al.* Combined PDK1 and CHK1 inhibition is required to kill glioblastoma stem-like cells in vitro and in vivo. *Cell Death Dis* 2014; **5**: e1223.
53 Akhurst RJ, Hata A. Targeting the TGFbeta signalling pathway in disease. *Nat Rev Drug Discov* 2012; **11**: 790–811.
54 Han G, Lu SL, Li AG, He W, Corless CL, Kulesz-Martin M *et al.* Distinct mechanisms of TGF-beta1-mediated epithelial-to-mesenchymal transition and metastasis during skin carcinogenesis. *J Clin Invest* 2005; **115**: 1714–1723.

Supplementary Information accompanies this paper on the Oncogene website (http://www.nature.com/onc)